Supporting Information

Arrangement Modulation of π-Stacked Columnar Assemblies of Octadehydrodibenzo[12]annulene: Substituent Effects of Peripheral Thienyl and Phenyl Rings

Ichiro Hisaki,[†*] *Keisuke Osaka,*[†] *Nobuaki Ikenaka*,[†] *Akinori Saeki,*[-‡] *Norimitsu Tohnai*,[†] *Shu Seki*,[‡♯] *Mikiji Miyata*[§]

[†] Department of Material and Life Science, Graduate School of Engineering, Osaka University, 2-1 Yamadaoka, Suita, Osaka 565-0871, Japan.

[‡] Department of Applied Chemistry, Graduate School of Engineering, Osaka University, 2-1 Yamadaoka, Suita, Osaka 565-0871, Japan.

[§] The Institute of Scientific and Industrial Research, Osaka University, 8-1 Mihogaoka, Ibaraki, Osaka 567-0047, Japan.

[‡] Present address: Department of Molecular Engineering, Graduate School of Engineering, Kyoto University, Nishikyo-ku, Kyoto-shi, Kyoto 615-8510, Japan.

Contents

1. Summary of crystal structures of [12]DBA 1

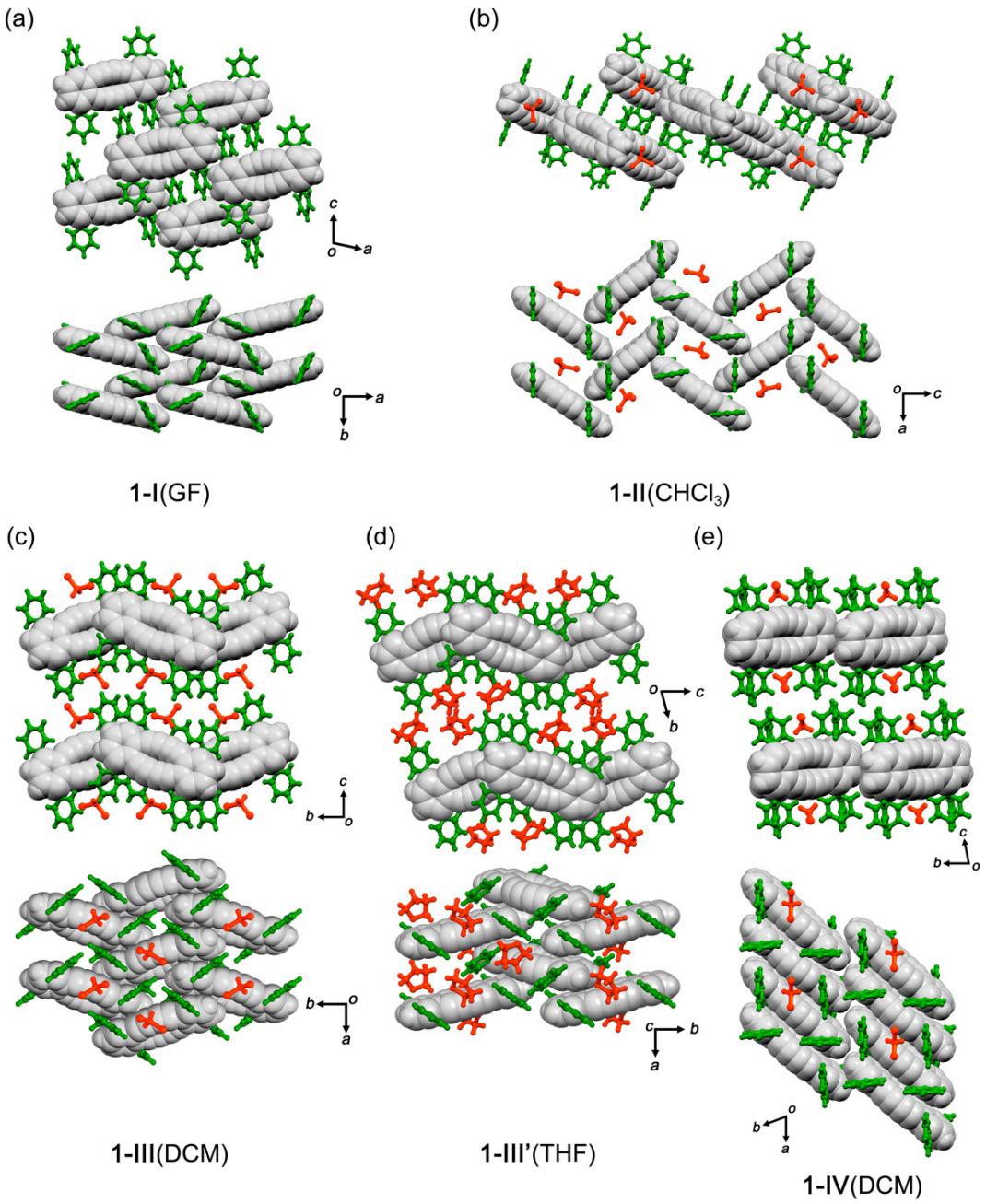

Figure S1. Packing diagrams of [12]DBA **1** in crystalline states.

2. Crystal structure of 2-II($CHCl_3$)

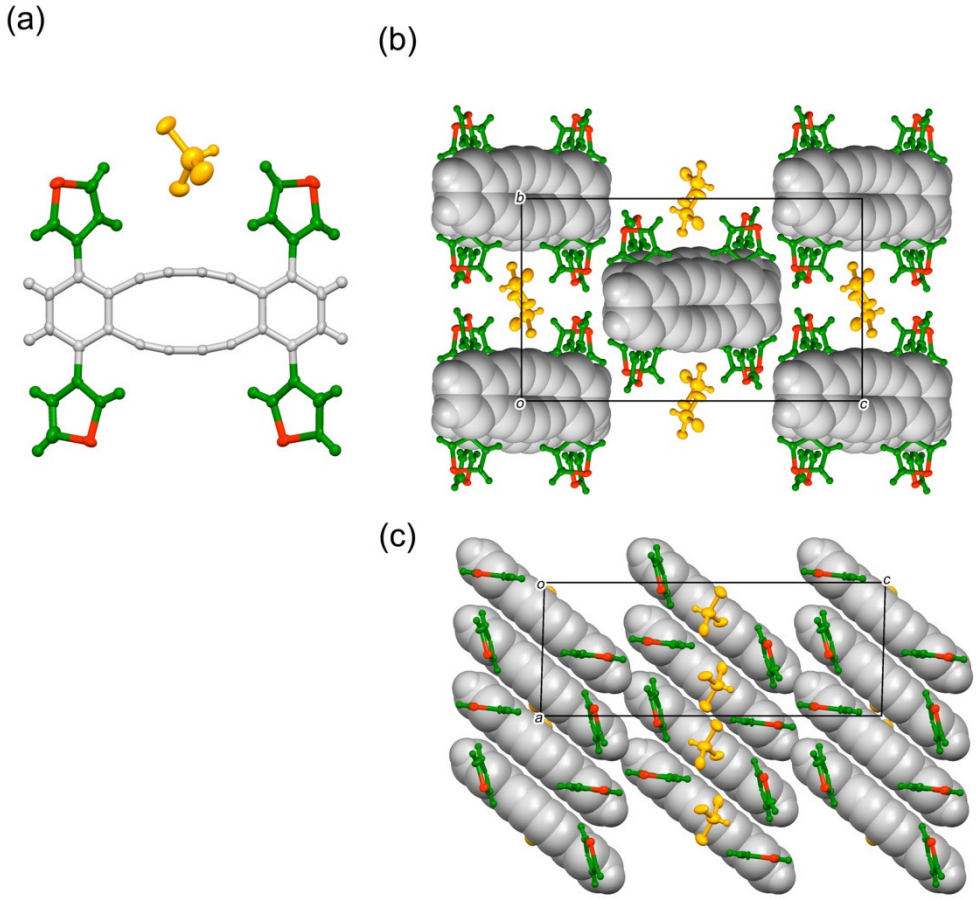

Figure S2. Crystal structure of **2-II**($CHCl_3$) (a) Anisotropic displacement ellipsoid plot with 50% probability. (b,c) Packing diagrams viewed from the *a* and *b* axes, respectively.

3. Thermal analyses of 2-I(GF), 2-II(THF), 2-II(DMF), and 2-II(NitroBn)

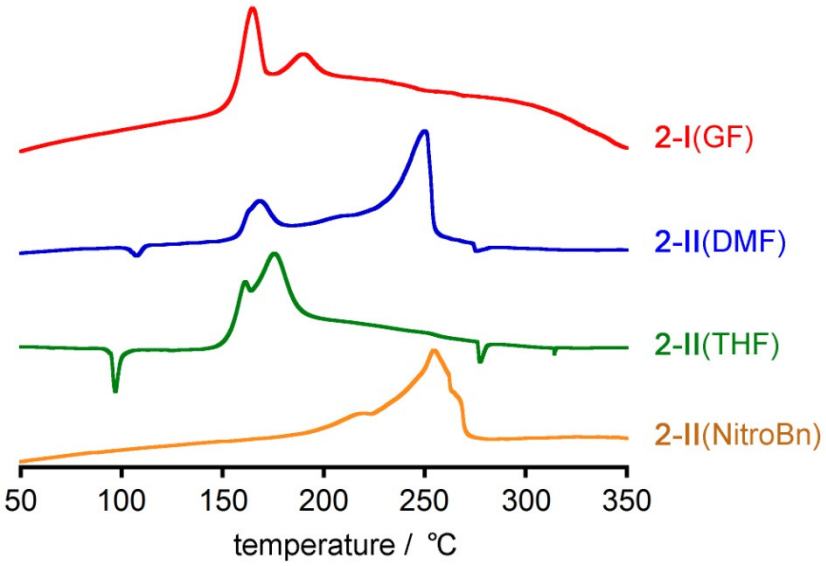

Figure S3. Differential scanning calorimetry (DSC) analysis of **2-I**(GF), **2-II**(DMF), **2-II**(THF), and **2-II**(NitroBn).

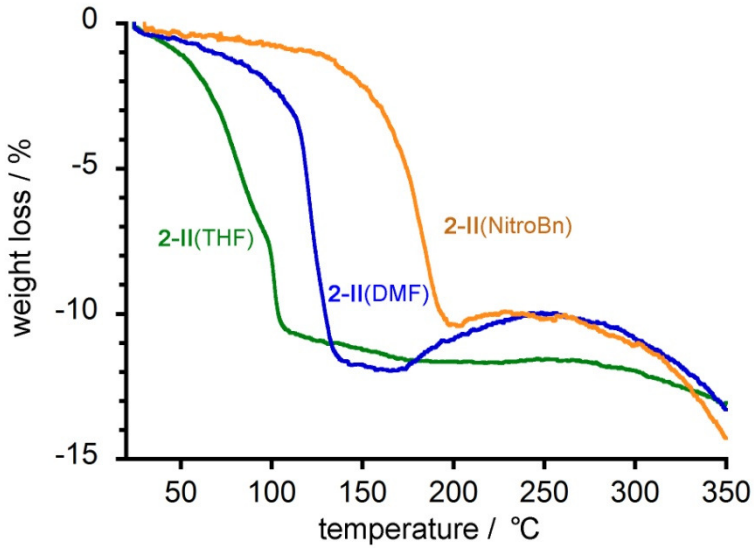

Figure S4. Thermal gravimetric (TG) analysis of **2-II**(DMF), **2-II**(THF), and **2-II**(NitroBn).

4. Structural transition of 2-II(DMF) into 2-I(GF) by guest desorption

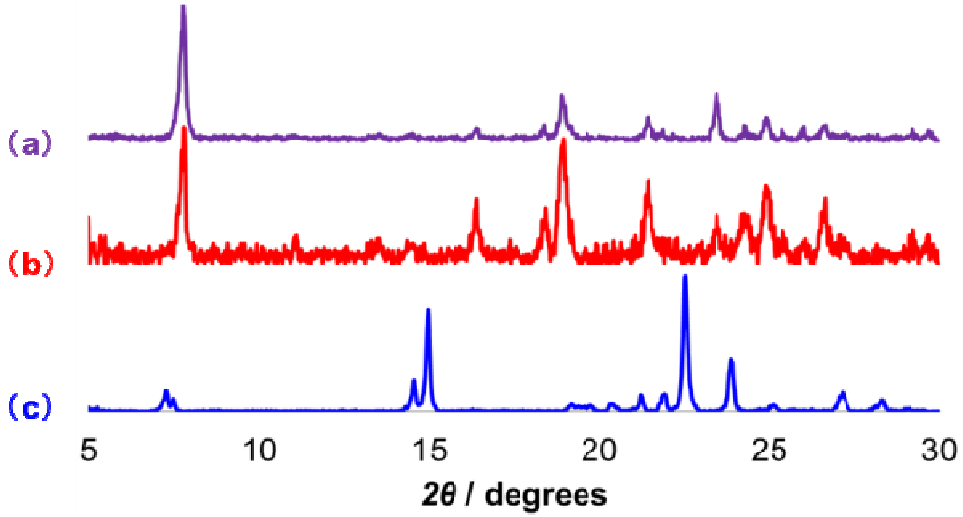

Figure S5. Powder X-ray diffraction patterns of (a) **2-I**(GF), (b) **2-II**(DMF) after guest desorption, and (c) **2-II**(DMF) as formed.

5. Theoretical calculation on [12]DBAs 1 and 2

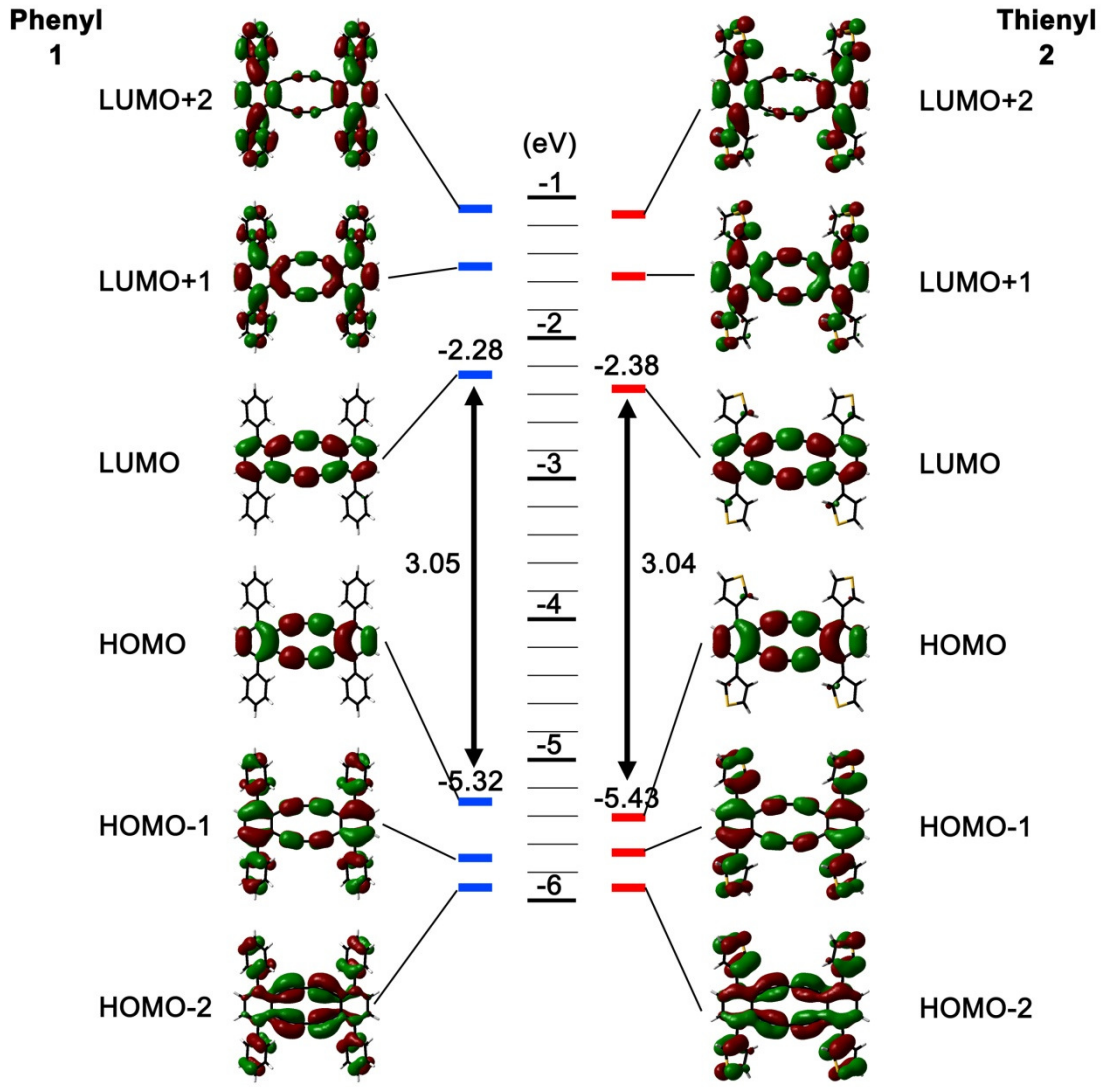

Figure S6. Energy levels of selected frontier molecular orbital of [12]DBAs **1** (left) and **2** (right).

6. Optical properties of [12]DBAs 1 and 2

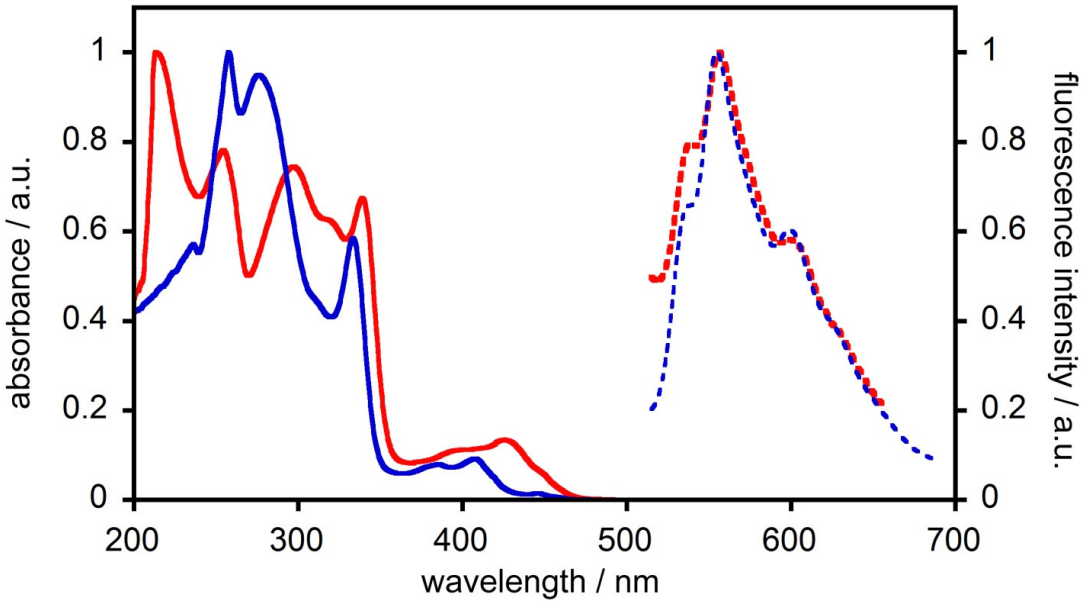

Figure S7. UV-vis (solid line) and fluorescence (dash line) spectra of [12]DBAs **1** (blue) and **2** (red) in chloroform. Absorbance and fluorescence intensity are normalized.

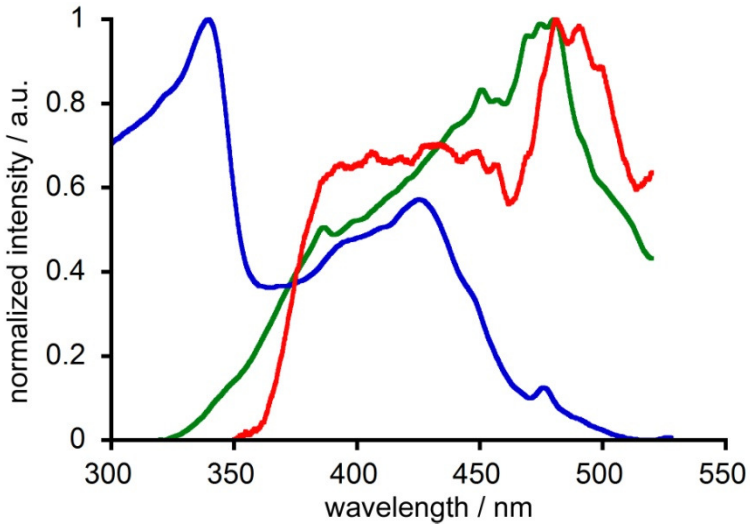

Figure S8. Excitation spectra of bulk crystals of **2-I**(GF) (green) and **2-II**(DMF) (red), as well as **2** in chloroform (blue) monitored at fluorescence maximum wavelength.

7. ^{1}H and ^{13}C NMR spectra of newly synthesized compounds

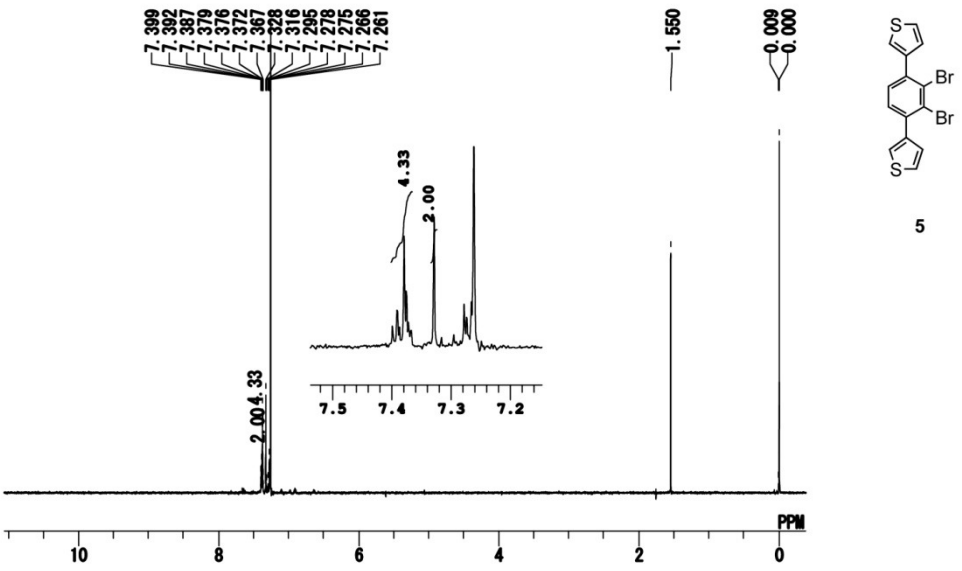

Figure S9. ^{1}H NMR (400 MHz, $CDCl_3$) spectrum of **5**.

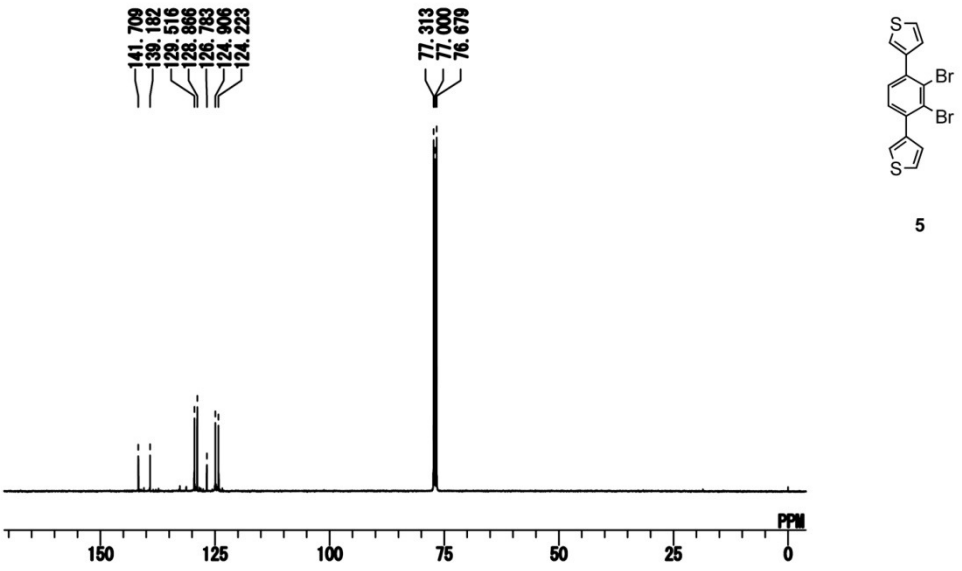

Figure S10. ^{13}C NMR (100 MHz, $CDCl_3$) spectrum of **5**.

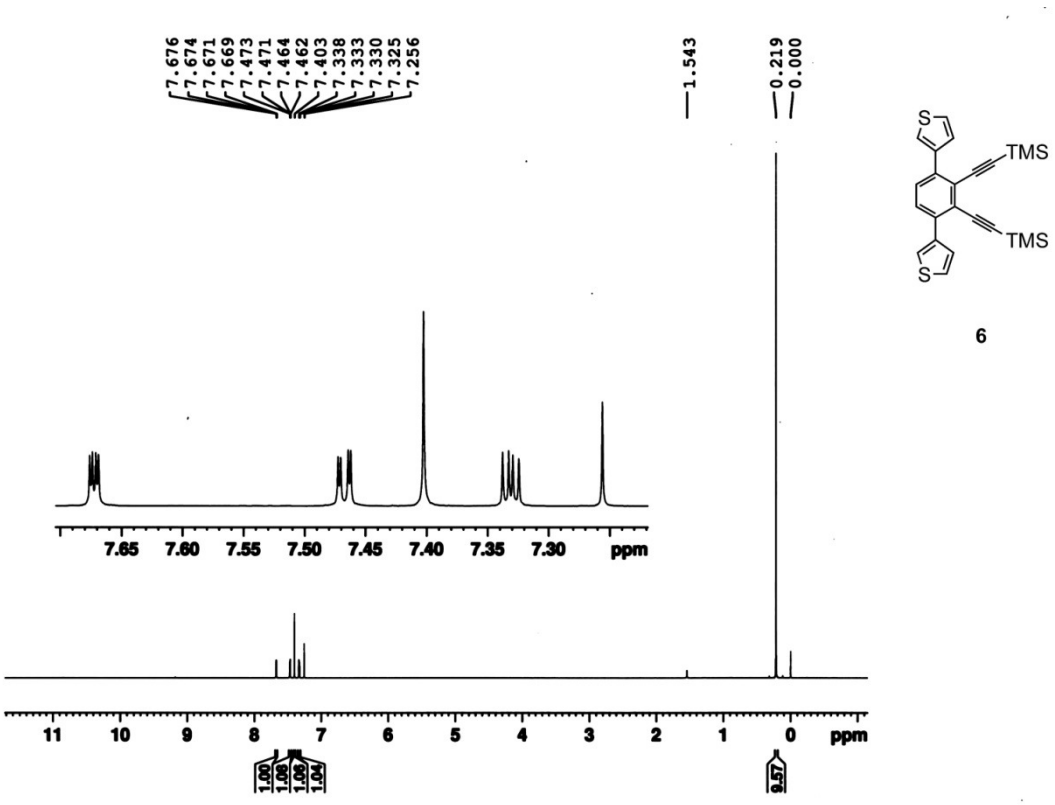

Figure S11. ^{1}H NMR (400 MHz, $CDCl_3$) spectrum of **6**.

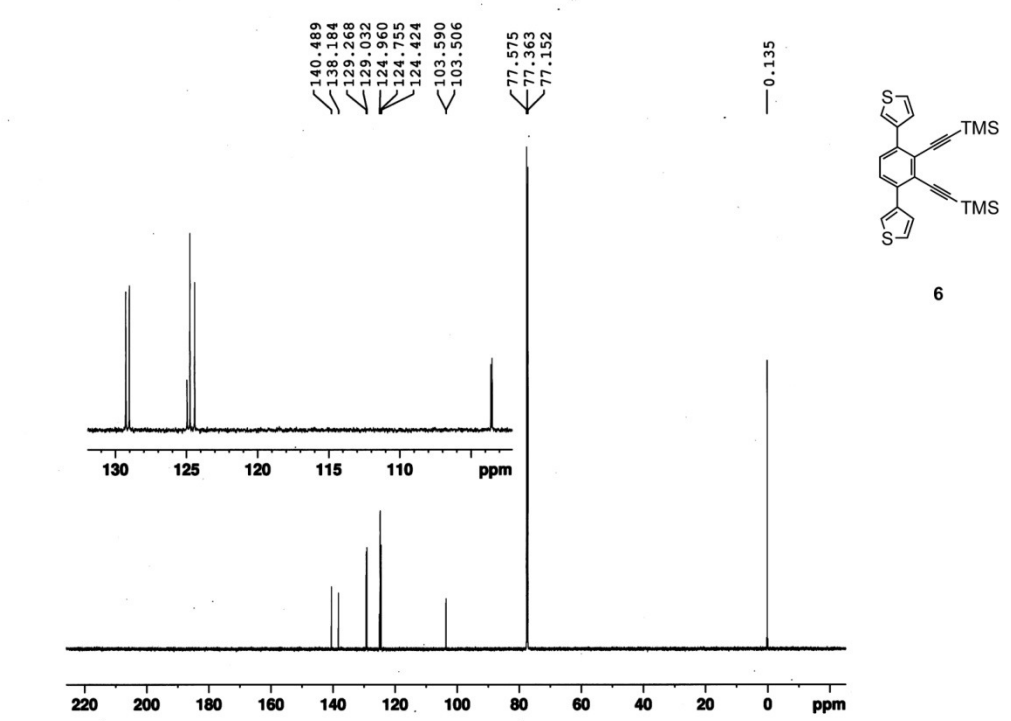

Figure S12. ^{13}C NMR (150 MHz, $CDCl_3$) spectrum of **6**.

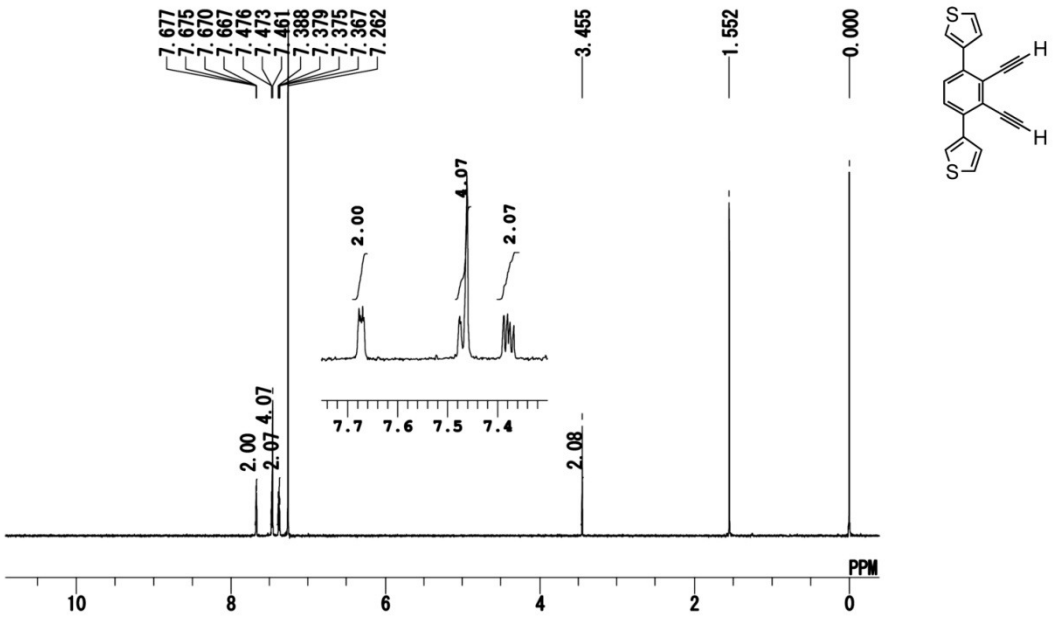

Figure S13. ^{1}H NMR (400 MHz, $CDCl_3$) spectrum of the precursor.

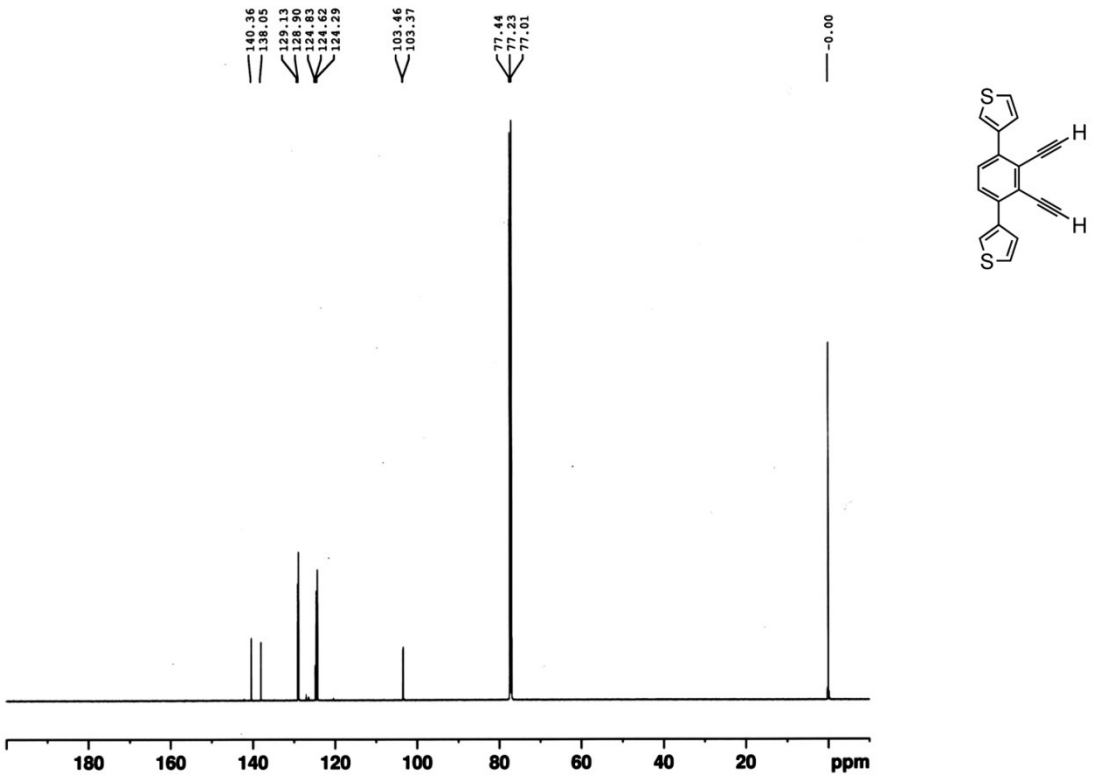

Figure S14. ^{13}C NMR (150 MHz, $CDCl_3$) spectrum of the precursor.

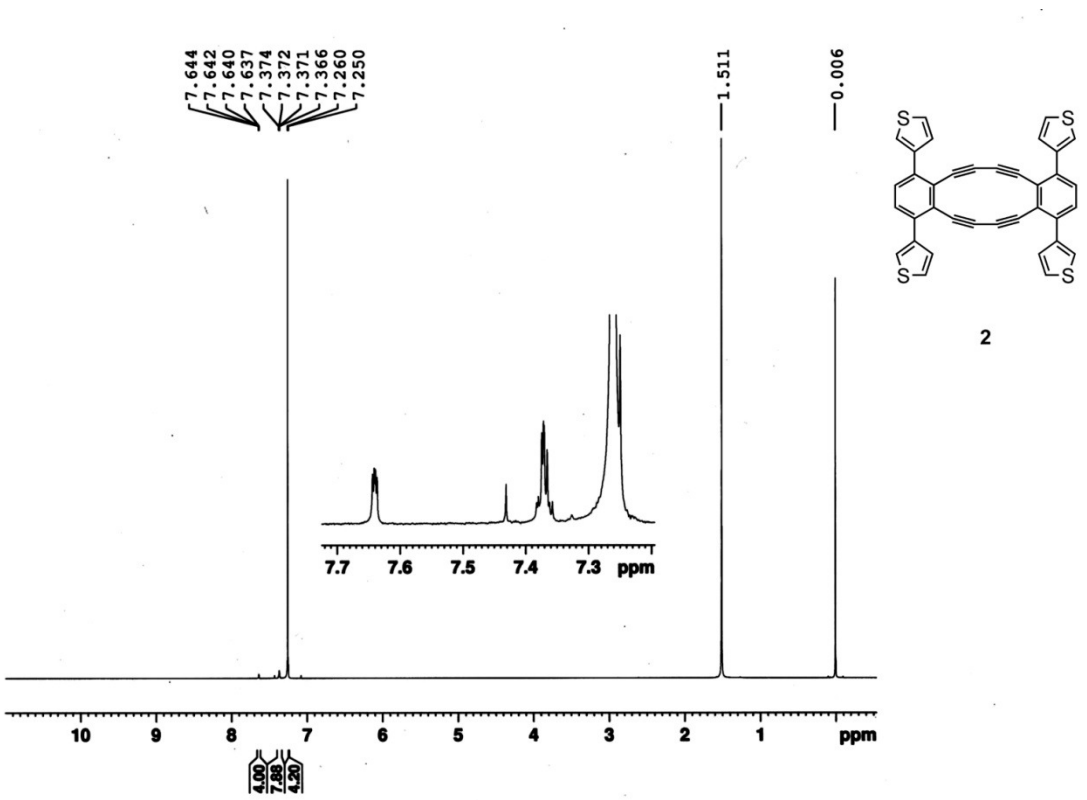

Figure S15. ^{1}H NMR (600 MHz, $CDCl_3$, 40 °C) spectrum of [12]DBA **2**.

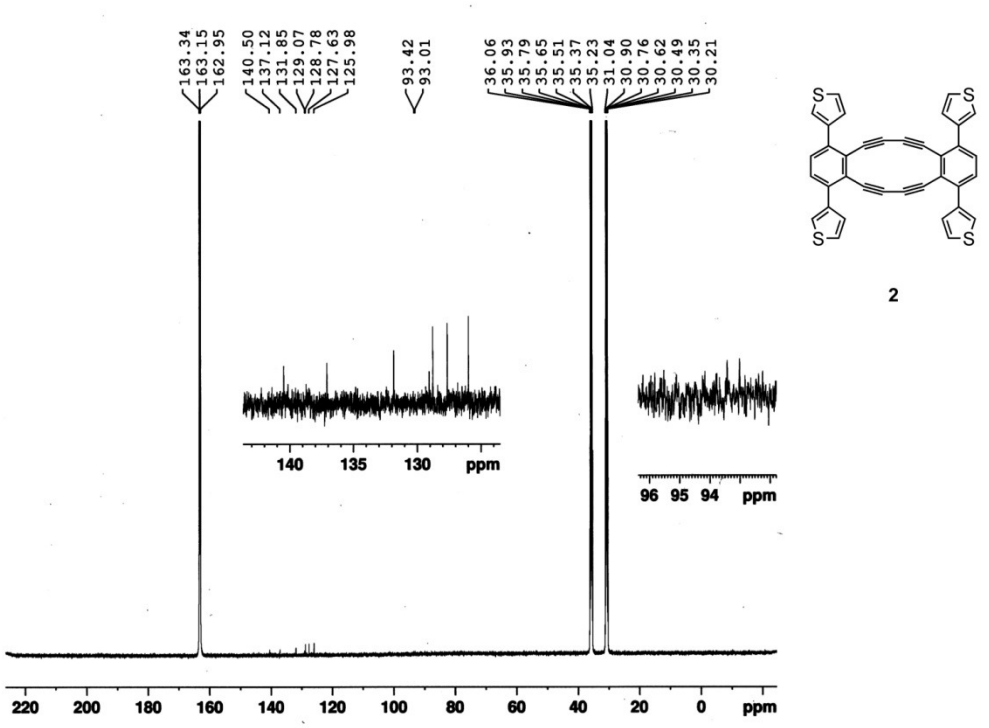

Figure S16. ^{13}C NMR (150 MHz, DMSO-d_6, 50 °C) spectrum of [12]DBA **2**.

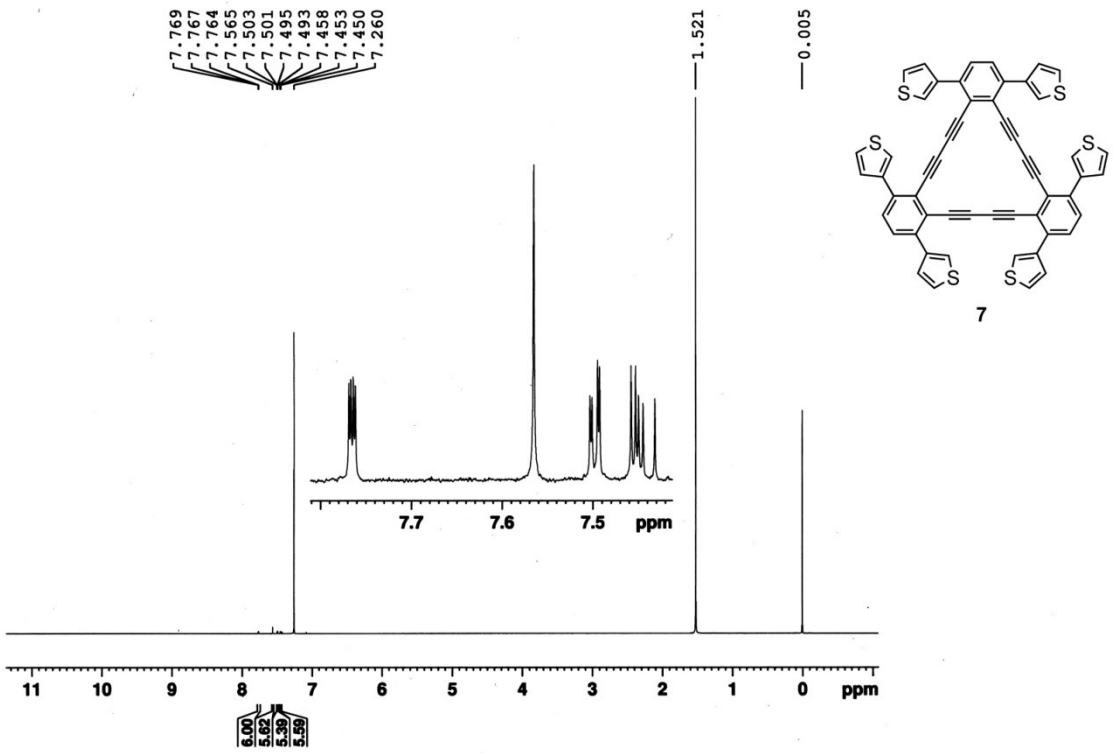

Figure S17. ^{1}H NMR (600 MHz, $CDCl_3$, 40 °C) spectrum of [18]DBA **7**.

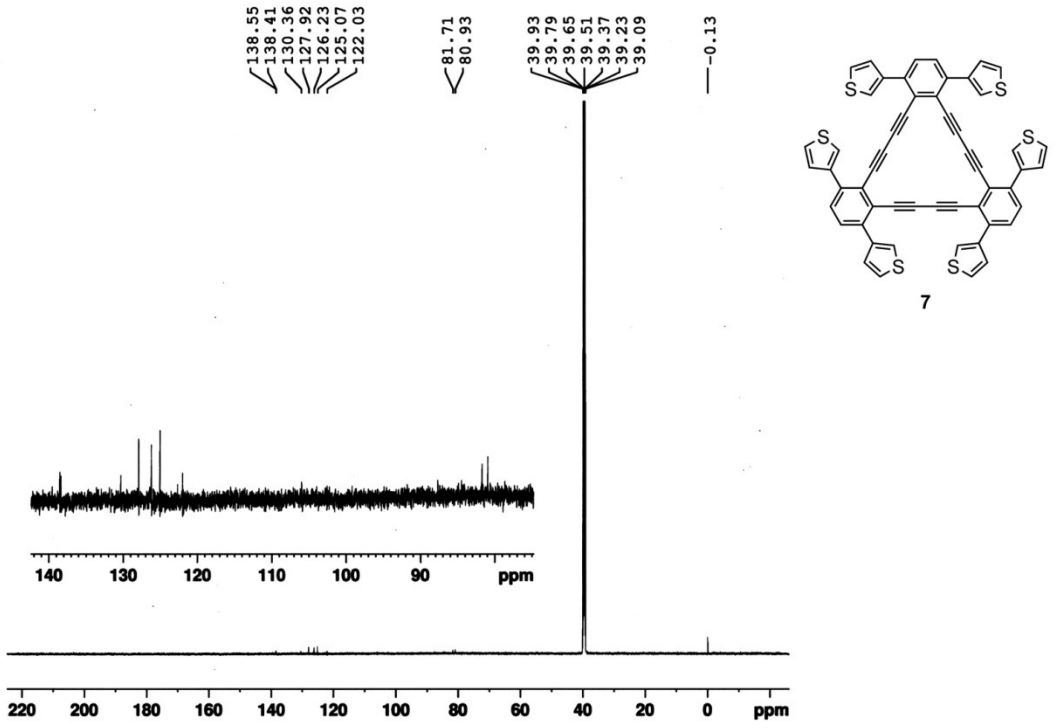

Figure S18. ^{13}C NMR (150 MHz, DMSO-d_6, 50 °C) spectrum of [18]DBA **7**.